Perturbation Method for Transonic Flows about Oscillating Airfoils

R.M. Traci,* E.D.Albano,* and J.L. Farr Jr.†
Science Applications, Inc., El Segundo, Calif.

A theory and numerical solution method are presented for the problem of two-dimensional unsteady transonic flow about thin airfoils undergoing harmonic oscillation. The theory is based on a treatment of the unsteady flow as a small perturbation on the nonlinear steady flow. The coupled governing equations for the steady and unsteady perturbation potentials are of mixed elliptic/hyperbolic type, and are solved by use of the mixed differencing, line relaxation technique of Murman and Cole. Detailed steady and unsteady results are compared to available data and more exact numerical calculations.

I. Introduction

A BASIC reason for studying unsteady flows is the prediction of the effect of unsteady aerodynamic forces on a flight vehicle. The transonic speed regime is particularly important in this respect for the same physical reason that drag and other steady forces are generally higher than in subsonic or supersonic speed regimes. Another characteristic of transonic flows is the potentially large phase lag between boundary motion and induced unsteady pressures. These effects tend to increase the likelihood of aeroelastic instabilities, so that transonic speeds are most critical for aircraft flutter. There is a clear and present need for accurate and efficient predictive techniques for unsteady transonic airloads. This need motivated the investigation of the perturbation method for transonic flows about oscillating airfoils presented in this paper.

The physical mechanism underlying the buildup of pressure amplitudes and phase lags has been described by Landahl,[1] by considering the propagation of a low-frequency acoustic disturbance. The upstream-facing portion of the disturbance (the "receding wave") travels at a rate that is essentially the difference between freestream speed and the sound speed. In a transonic flow, this speed is so slow that acoustic disturbances may interact and build up to a finite amplitude. In order to describe the phenomenon, the steady or low-frequency unsteady equations must necessarily be nonlinear, thereby providing the essential difficulty in the analysis of transonic flow. It has been pointed out by Rott,[2] Landahl,[3] and others, however, that the unsteady equations may be linearized and uncoupled from the mean steady flow for high frequency disturbances near Mach 1. These so-called "sonic theories" have been developed for both two- and three-dimensional wings by a number of investigators.[2-4] Many of these classical studies of the high-frequency equation are summarized in Landahl's monograph.[1] It is often the case, however, that the nonlinear low-frequency regime is of greater practical importance for aircraft flutter. Fortunately, a linear system can be recovered for low-frequency transonic flow, as demonstrated by Landahl,[3] by expanding the unsteady flow as a small perturbation about the nonuniform steady flow. The linear equation remains quite formidable since various coefficients are functions of the nonlinear steady flow, so that numerical solution procedures, of which the present work is one, are indicated.

Analytical or semianalytical approaches to the solution of the unsteady flow, based on this linearization about the steady flow, have been presented recently. Stahara and Spreiter[5] and Isogai[6] have applied the "local linearization" method, developed for steady, near sonic flows, to the nonuniform unsteady system. The approach is promising, but its application to general supercritical flows is questionable.

Of more practical interest for general applications are the numerical approaches, which have become highly developed for steady flows in recent years. Two basic finite-difference techniques have been used, known generally as time-dependent methods and relaxation methods. The time-dependent methods solve the complete set of conservation equations or the unsteady full potential equation by forward differencing in time. This approach has been applied to the calculation of steady flows as the steady limit of the time-dependent solution. The method can handle mixed flows and shocks within the accuracy of the finite-difference mesh.[7] Time-dependent calculations of flows about two-dimensional airfoils oscillating at super-critical Mach numbers have been reported by Magnus and Yoshihara.[8] Such calculations are very important since they involve no inherent limiting assumption, but they are quite expensive computer timewise. In a related method, Beam and Warming[9] present finite-difference solutions of the exact Euler equations for impulsive airfoil motions from which they develop indicial functions for small perturbation oscillations about the linear steady state. Ballhaus and Lomax[10] have presented time-accurate solutions of the low-frequency unsteady small disturbance potential equation. Recent applications of the method[11] indicate that it could be a very efficient approach to the oscillating airfoil problem.

Another promising technique for both steady and unsteady flows, which must be considered in a separate classification, is the finite-element method. The method has been applied to the oscillating airfoil problem by Bratanow and Ecer[12] for compressible flow and recently by Chan and Brashears[13] for transonic flows.

The other class of numerical techniques, which have received wide application to steady transonic flows,[14,15] are the relaxation methods. Ehlers[16] and the present authors[17] have reported the application of relaxation methods to unsteady transonic flows about harmonically oscillating airfoils. These methods apparently are similar, except that the work presented here concentrates in a consistent manner, from formulation through results, on the low-frequency regime. In the approach, the flow is considered as a small perturbation on the steady flow which results in a pair of boundary value problems for the steady and first-order unsteady perturbation

Presented as Paper 75-877 at the AIAA 8th Fluid and Plasma Dynamics Conference, Hartford, Conn., June 16-18, 1975; submitted July 18, 1975; revision received Jan. 14, 1976. Work sponsored by Air Force Flight Dynamics Laboratory, Wright-Patterson Air Force Base, Ohio, Contract F33615-74-C-3094.

Index categories: Nonsteady Aerodynamics; Subsonic and Transonic Flow.

*Staff Scientist. Member AIAA.

†Staff Scientist.

potentials. The equation for the steady flow is just the nonlinear small disturbance potential equation. The first order unsteady equation is linear, and for the harmonic boundary disturbances considered, its reduced wave equation form is of mixed elliptic/hyperbolic type, depending upon the nature of the steady solution. Both steady and unsteady equations are solved by the mixed differencing line relaxation procedure first introduced for steady flows by Murman and Cole.[14]

Since the approach and numerical solution procedure have been reported in detail elsewhere, they are but summarized in Sec. II., which follows. The present paper concentrates on presenting results generated by use of the method, and on verifying the accuracy of the method for airfoils with practical shapes and unsteady amplitudes. To this end, results are presented in Sec. III. for a NACA 64A410 airfoil oscillating in pitch at a freestream Mach number of 0.72 and for a NACA 64A006 airfoil with control surface oscillation for the entire transonic range from fully subsonic to fully supersonic flow. The NACA 64A410 results are compared in detail to the "exact" numerical results of Magnus and Yoshihara[8] with discussion of the accuracy of the small perturbation approach. Calculations of unsteady aerodynamic coefficients for the NACA 64A006 are presented for reduced frequencies up to 0.2 with comparison to the experimental data of Tijdeman et al.[18,19] Calculations showing the effect of mean airfoil angle of attack on unsteady results also are discussed. The final section summarizes study results and conclusions.

II. Formulation and Solution Procedure

Small disturbance theory is the principal analytical tool for all speed ranges, and the transonic speed range is no exception. The general theory including the unsteady small perturbation approach used in this work is summarized in Sec. II. A. The approach achieves a linear unsteady system at the cost of some complication of the governing equation. The required numerical solution method for both the steady and unsteady system is described in Sec. II. B.

A. Small Perturbation Approach to Unsteady Transonic Flow

The problem of interest is two-dimensional flow about an airfoil oscillating in shape, angle of attack, or flap angle in the transonic flow speed range. Of particular interest are the steady and unsteady aerodynamic forces on the airfoil for use in flutter studies. The airfoil geometry, flowfield schematic, and coordinate definition are given in Fig. 1. Rectangular coordinates (x,y) are fixed to the airfoil leading edge, and U, M_∞, a_∞ are the freestream velocity, Mach number, and sound speed, respectively. The airfoil has a thickness ratio δ, which is the airfoil maximum thickness divided by its chord c, and an angle of attack α. The assumption is made that $\delta << 1$ and α is of the same order of magnitude as δ. Also, the oscillatory motion of the airfoil is assumed to be described by a small nondimensional displacement $\epsilon << \delta$ and a reduced frequency $k=\omega c/U$ based on airfoil chord, where ω is the frequency of oscillation.

Assuming inviscid, isentropic flow, the problem can be reduced to the solution of a single equation for a velocity potential plus the tangency boundary condition on the airfoil surface. As is well-known, the derivation of a small disturbance theory for transonic flows requires a singular perturbation approach. The following scaling is introduced:

$$\bar{x}=x/c \qquad \bar{y}=[(1+\gamma)\delta M_\infty^2]^{1/3}(y/c)$$

$$\bar{t}=\frac{[(1+\gamma)\delta M_\infty^2]^{1/3}}{M_\infty^2}\frac{U}{c}t \tag{1}$$

and the total potential is expanded about the uniform flow;

$$\psi=Uc\bar{x}+\frac{\delta^{1/3}Uc}{[(1+\gamma)M_\infty^2]^{1/3}}\bar{\phi}(\bar{x},\bar{y},\bar{t})+\ldots \tag{2}$$

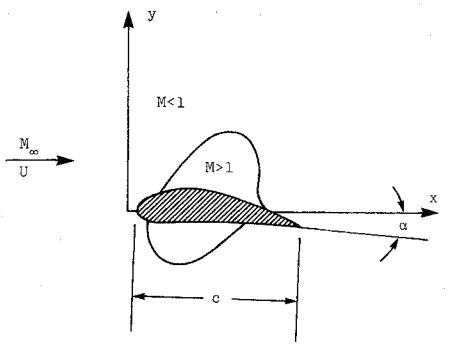

Fig. 1 Schematic of airfoil geometry and transonic flowfield.

Retaining all terms to leading order in the total potential equation and boundary condition results in the following form for the unsteady small perturbation system:

$$(K-\bar{\phi}_{\bar{x}})\bar{\phi}_{\bar{x}\bar{x}}+\bar{\phi}_{\bar{y}\bar{y}}=2\bar{\phi}_{\bar{x}\bar{t}}+(k/\Omega)\bar{\phi}_{\bar{t}\bar{t}} \tag{3}$$

where the transonic similarity parameters are:

$$K=\frac{(1-M_\infty^2)}{[(1+\gamma)\delta M_\infty^2]^{1/3}} \qquad \Omega=\frac{M_\infty^2}{[(1+\gamma)\delta M_\infty^2]^{1/3}}k$$

with boundary conditions

$$\bar{\phi}_{\bar{y}}=\left(\frac{\partial}{\partial\bar{x}}+\frac{k}{\Omega}\frac{\partial}{\partial\bar{t}}\right)f_{u,l}(\bar{x},\bar{t})$$

$$\text{on } \bar{y}=\pm 0 \qquad 0<x<1 \tag{4}$$

$$\left[\bar{\phi}_{\bar{x}}+\frac{k}{\Omega}\bar{\phi}_{\bar{t}}\right]=0 \quad \text{on } \bar{y}=0 \qquad \bar{x}>1 \tag{5}$$

$$\bar{\phi}_{\bar{x}}^2+\bar{\phi}_{\bar{y}}^2\to 0 \quad \text{as } \bar{x}^2+\bar{y}^2\to\infty \tag{6}$$

where $f_{u,l}$ is the unsteady airfoil shape function [Eq. (7)] on the upper and lower surfaces, respectively, and where [ ] denotes a jump between 0^- and 0^+. It is noted that the airfoil tangency boundary condition [Eq. (4)] and Kutta condition [Eq. (5)] are applied in the small disturbance manner on $y=0$.

The system of Eqs. (3-6) provides a formulation of the unsteady airfoil problem in the nonlinear domain, which includes flowfields with shocks. Equation (3) contains the usual small disturbance approximation to shock jump conditions, which provide the lowest order approximation to the Rankine-Hugoniot shock relations. Certain terms in the preceding system are in bold-face type, since they may be omitted for a low frequency $[k\sim O(\delta^{2/3})]$ approximation. The low-frequency approximation results in significant numerical advantages when solved by a time-dependent technique, as pointed out recently by Ballhaus and Lomax.[10] Time-dependent numerical approaches to the solution of the previous system have yet to be fully exploited for the unsteady aerodynamics problem.

The approach presented herein for solving the nonlinear system given in Eqs. (3-6) is to expand the perturbation potential function in terms of the unsteady boundary disturbance $\epsilon << 1$. From this point on, the tilde $(\sim)$ will be dropped, with the understanding that all variables are scaled variables. Harmonic boundary disturbances are explicitly treated:

$$f(x,t)=f_0(x)+\epsilon f_1(x)e^{i\Omega t} \tag{7}$$

and the perturbation potential is expanded as follows:

$$\phi(x,y,t)=\phi^0(x,y)+\epsilon\phi^1(x,y)e^{i\Omega t}+\ldots \tag{8}$$

Substituting this into the perturbation potential equation plus boundary conditions, and combining terms, results in the following pair of boundary value problems for ϕ^0 and ϕ^1, respectively. (In the text that follows, the superscript has been dropped from ϕ^1.)

$$\left.\begin{aligned} &(K-\phi_x^0)\phi_{xx}^0+\phi_{yy}^0=0 \\ &\phi_y^0=f_0'(x) \qquad \text{on } y=\pm 0 \qquad 0\le x\le 1 \\ &[\phi_x^0]=0 \qquad \text{on } y=0 \qquad x>1 \\ &(\phi_x^0)^2+(\phi_y^0)^2\to 0 \qquad \text{as } x^2+y^2\to\infty \end{aligned}\right\} \tag{9}$$

and

$$\left.\begin{aligned} &(K-\phi_x^0)\phi_{xx}+\phi_{yy}-(\phi_{xx}^0+2ik\Omega)\phi_x+k\Omega\phi=0 \\ &\phi_y=f_\epsilon'+ikf_\epsilon \qquad \text{on } y=\pm 0 \qquad 0\ge x\le 1 \\ &[\phi_x+ik\phi]=0 \qquad \text{on } y=0 \qquad x>1 \\ &(\phi_x)^2+(\phi_y)^2\to 0 \qquad \text{as } x^2+y^2\to\infty \end{aligned}\right\} \tag{10}$$

System 9 is recognized as the usual formulation for steady transonic flow, and system 10 is the formulation for the unsteady perturbation thereof. It is noted that the governing equation for ϕ is linear, but of the same mixed elliptic/hyperbolic type as the steady solution. It also is noted that ϕ is, in general, complex, thereby permitting phase shifts between the field quantities and the boundary disturbance.

The steady and unsteady formulations both provide for jumps in their respective velocity perturbations across shocks. The jump conditions for the steady system have been discussed by numerous authors, and can be written as

$$[(\phi_{x_1}^0+\phi_{x_2}^0)/2-K]<\phi_x^0>^2=<\phi_y^0>^2 \tag{11}$$

where $<\ >$ denotes jump in the quantity across the shock, and subscripts 1,2 denote conditons upstream or downstream of the shock. The corresponding conditions contained in the unsteady formulation, assuming the shock remains fixed, ϵ, can be shown to be the following:

$$<(K-\phi_x^0)\phi_x>^2=[(\phi_{x_1}^0+\phi_{x_2}^0)/2-K]<\phi_y>^2 \tag{12}$$

Thus, shocks in the steady field require corresponding shocks in the unsteady perturbation field, which in effect result in harmonic changes in shock strength. It should be noted that changes in shock position are expected to this same order in ϵ; however such shock oscillations are neglected in the present study.

The main physical quantities of interest are the pressure coefficient and airfoil force coefficients. The pressure coefficient, defined in the usual manner, is given by:

$$C_p=\frac{\delta^{2/3}}{[(1+\gamma)M_\infty^2]^{1/3}}(\bar{C}_p^0+\epsilon\bar{C}_p e^{i\Omega t}) \tag{13}$$

where the steady and unsteady scaled pressure coefficients are given to leading order in the small disturbance approximation by

$$\bar{C}_p^0=-2\phi_x^0,\ \bar{C}_p=-2(\phi_x+ik\phi) \tag{14}$$

The formulation of the boundary value problem is essentially complete, with the exception of the practical matter of setting the boundary conditions away from the airfoil, which depends on the particular problem; free-field, wind-tunnel walls, etc. For the subsonic free-air calculations reported here, an asymptotic farfield solution to Eq. (10) has been developed[17] and is utilized to fix a Dirichlet boundary condition on the boundary of the finite-difference grid. For calculations with a supersonic freestream, a characteristic condition for outgoing characteristics of the unsteady system [Eq. (10)] also has been developed[20] and is applied on the grid boundary.

B. Finite-Difference Solution Method

The numerical solution procedure for boundary value problems for the steady and unsteady perturbation potential, given previously, is based on the mixed differencing line relaxation procedure developed by Murman, Cole, and Krupp.[14,15] They pointed out the essential ingredient for the success of relaxation procedures for the steady transonic potential equation. The key to the approach is to account for the local nature of the flow (elliptic in subsonic regions, hyperbolic in supersonic regions) in the finite-difference approximation to the governing equations. The solution method used in the present work for the steady perturbation potential ϕ^0 is patterned after the method for general lifting airfoils developed by Krupp.[15] The version of this technique, implemented for the unsteady perturbation, is described here.

In the numerical scheme, a rectangular mesh with general grid line spacing, is overlayed on the solution field in physical x,y coordinates. Uneven grid spacing makes it possible to concentrate grid points near the airfoil slit, and in regions where rapid changes in the potential or its derivative (wing leading edge, shocks, etc.) are expected, and to expand the grid in a regular manner out to the boundaries of the mesh. The required solution for ϕ^0, which does not depend on ϕ, is solved independently on the same or a more refined grid, and the resulting solution is stored on magnetic tape. The converged solution so obtained then is used in the solution process for the corresponding ϕ. This approach has the benefit that ϕ^0 need not be regenerated for each unsteady boundary disturbance or reduced frequency of interest.

The local nature of the equation at each grid point is determined by the corresponding value of $(K-\phi_x^0)_{i,j}$ at the same grid point. Then if $K-\phi_x^0>0$ (elliptic) the x derivatives of ϕ are center differenced, and if $K-\phi_x^0>0$ (hyperbolic) the x derivatives are backward differenced. Near the sonic line at "parabolic points," the center difference form for the x derivatives of ϕ are used. This form of the parabolic point operator is used in both the steady and unsteady solutions and is patterned after Krupp,[15] who found that it has somewhat better stability properties than the simpler form ($\phi_{yy}=0$) used by Murman. Finally, it is noted that shocks that develop in the solution field are not accorded any special treatment. This so-called "nonconservative" differencing[21] was used in the present study, since it is well-known that it results in better agreement with experimental data, thereby accounting for viscous effects in an ad hoc manner.

Using the difference forms described, the finite-difference equations are set up for each column ($x=$const) in the grid. Appropriate finite-difference approximations are made for the body boundary condition, Kutta condition, and farfield boundary to effectively close the system of equation. The resulting sequence of linear algebraic equations is solved by Gaussian elimination. After each column is solved, it is relaxed with a variable relaxation factor, depending on the local nature of the solution. This process is repeated for each column in turn, sweeping the grid from left to right until the change in ϕ for all grid points during one grid sweep is less than some arbitrary small amount. Iteration also is required on the unknown airfoil circulation, which is always overrelaxed and which is updated along with the farfield at regular intervals. A grid-halving routine has been implemented with considerable improvement in the efficiency of the method. Complete details of the method can be found in Ref. 17.

The method summarized previously is capable of and has been used to calculate a wide range of general lifting airfoils in the transonic speed regime for either subsonic or supersonic freestreams and with free air or wind-tunnel farfields.

Various rigid body modes of oscillation, including pitch, plunge, or control surface rotations, have been considered for a range of reduced frequencies. Execution times depend upon the combination of similarity parameters (K,Ω), grid design, and degree of convergence, but are typically 2 to 3 min of CDC 6600 time for acceptable accuracy. Stability problems have been encountered for a combination of Mach numbers very near 1 and/or increasing reduced frequency. A preliminary stability analysis indicates that the instability is related to the inability of the finite-difference grid to resolve short wavelength (λ_u) upstream facing waves. That is, the requirement that $\lambda_u \simeq (1-M)/k > \Delta x$ is not satisfied as M approaches 1 and k increases. If this occurs over a large enough region of the grid, an instability is likely. It is noted that expansion of the grid as used here most likely compounds the problem. Practical limitations on the application of the method due to this instability are discussed in context of the results presented in the next section.

III. Calculated Results

Results are presented in this section for a NACA 64A410 airfoil oscillating in pitch and a symmetric NACA 64A006 with oscillating control surface hinged at the ¾ chord line. Before proceeding with the comparisons, some comments concerning interpretation of the results and various computational details are in order.

In all of the unsteady calculations to follow, the low-frequency approximation, which involves dropping underlined terms in the preceding formulation, was used. This is expected to have no bearing on the results for the reduced frequency range $(k \leq 0.2)$ considered. The forms of the unsteady perturbation to the airfoil slope distribution for pitch and control surface oscillations are, respectively,

$$f'_\epsilon = -1,\ 0 \leq x \leq 1 \tag{15}$$

$$f'_\epsilon = \begin{cases} 0, & 0 \leq x \leq x_f \\ -1, & x_f \leq x \leq 1 \end{cases} \tag{16}$$

where x_f is the hinge point. In the respective cases, the magnitude of the perturbation is α/δ or β/δ, where α and β are the amplitudes of the oscillating component of angle of attack or flap angle, respectively. The amplitudes of the resulting perturbations to the airfoil pressure coefficients in unscaled (C_p) or scaled $(\bar{C}_p)$ form are given by Eqs. (13) and (14). It is noted that the scaling used in Eq. (13) for the pressure coefficient, commonly known as Spreiter scaling, is a natural result of the nondimensionalization used here. No attempt has been made to modify the Mach number dependence in the scaling to provide better agreement with data or exact results, as often is done elsewhere.[15] Finally, it is noted that lift $(C_{\ell\alpha,\beta})$ and moment $(C_{m\alpha,\beta})$ and hinge moment $(C_{n\alpha,\beta})$ coefficients are calculated by a trapezoidal rule integration of the calculated pressure coefficient distributions.

In the present calculations, the refined grid (achieved by refining a coarse grid by the "grid halving" procedure) consisted of 48 points in the x direction and 47 points in the y direction. Over half (26) of the grid columns are on the airfoil, and grid rows are divided in a symmetric manner above and below the airfoil. The grid is expanded in a regular manner out to $x \simeq \pm 3$ and $y \simeq \pm 6$, at which point an analytic farfield expression is imposed as a boundary condition. As discussed below, the grid so defined is not altogether adequate for an airfoil with the bluntness, thickness, and camber of the NACA 64A410. Previous experience indicated that such a grid would provide relatively good results, so that no attempt was made at optimizing the grid structure for each case. In both steady and unsteady calculations, the iteration procedure was continued until the maximum change in potential, over all grid points, from one iteration to the next was less that $\sim 10^{-4}$. In each case, this resulted in a convergence of the airfoil circulation to better than 10^{-4}. Numerical tests have indicated that this degree of convergence provides reasonable accuracy.

A. NACA 64A410 Oscillating in Pitch at $M_\infty = 0.72$

Magnus and Yoshihara[8] (M – Y) recently have presented time-dependent calculations of the flow past a NACA 64A410 airfoil oscillating in pitch at Mach 0.72. Their highly refined numerical method is based on the full unsteady inviscid flow equations with kinematic boundary conditions fixed at the mean airfoil surface. These "exact" solutions provide a unique comparison for verification of the present approximate method. The nose bluntness, thickness, and camber of the airfoil, coupled with the mean and oscillating amplitude of angle of attack $(\alpha = 2° \pm 2°)$, provide a severe but practical test of both the small disturbance approximation and the linearized unsteady method.

Results for the steady pressure distributions for $\alpha_0 = 2°$ are presented in Fig. 2; pluses (+) and Δ indicate points computed by the present method and by M – Y, respectively. All in all, the comparison is moderately good with the exception of two anomalies: the shock description, and a "knee" in the small disturbance pressure distribution on the upper surface near the nose. Lifts predicted by both methods compare well, as do the lower surface pressure distributions. The shock calculated by the present method is farther forward, more diffuse, and weaker, which can be attributed to the relatively coarse grid and the use of the nonconservative differencing of the present method. It is believed that the shock description could be improved by the use of shock point differencing[21] or shock fitting,[22] as well as a denser gridwork in the region of the shock. However, it should be pointed out that the shock Mach number is about 1.3, which would indicate that the small disturbance shock description is not accurate. The other anomaly in the comparison which has some bearing on the linear perturbation results to follow is the sharp change in slope of the predicted pressure distribution near the nose. This behavior is not shown in the M – Y results. It is probably because of the approximation to the airfoil slope distribution used in the present method, as well as possible inaccuracy of

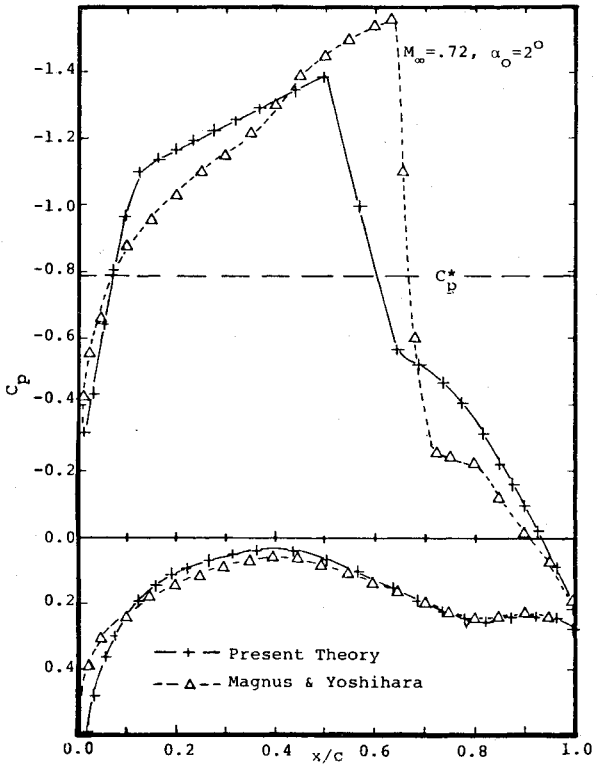

Fig. 2 Steady pressure distribution (NACA 64A410).

the small disturbance description of the rapid expansion of the flow about the nose of the airfoil.

Calculations of linearized unsteady perturbations about the steady flow described previously have been performed, and amplitudes of perturbations to the pressure coefficients due to a 2° pitch oscillation are shown in Figs. 3 and 4 for the steady $k=0$ and low-frequency unsteady $k=0.2$ cases. The results of the present theory again are compared to results deduced from the M – Y calculations. The M – Y results for both nose-up (2°→4°) and nose-down (2°→0°) motion are shown to give some indication of inherent nonlinearity. It is noted that the nonlinear behavior is surprisingly small on the supercritical upper surface and surprisingly large on the subcritical lower surface. The present results for the lower surface compare well with the M – Y results. The comparison in each case for the upper surface is consistent with the deficiencies in the present result for the steady flow being perturbed. The discrepancy at the shock is to be expected, since the M – Y calculations show significant shock excursions (indicated on the graphs), which are not accounted for in the present work. The linearized results show a peak suction through the steady shock, which is an attempt by the linear theory to account for the strengthening (or weakening) of the shock due to a nose-up (or nose-down) pitch perturbation. The present results also show an as yet unexplained decreased suction (dip) near the $x=0.1$ station which corresponds to the "knee" in the steady pressure distribution discussed previously.

The results of interest for flutter applications are the perturbations to the integrated airfoil forces. Table 1 compares the increment in lift and moment coefficient in steady flow as the angle of attack increases from 0° to 2° and from 2° to 4°. Also compared are the linear parts of the oscillating coefficients for the $k=0.2$ pitching oscillation with 2° amplitude. The good agreement in each case would seem to indicate that the linearized perturbation method provides a useful approximation to the oscillatory forces for quasisteady and low-frequency oscillations. It may be noted that for this example the ratio of oscillatory amplitude (at 2°) to the thickness is $\epsilon=0.35$, which is a relatively large perturbation.

The M – Y results for $k=0.2$ shown in Table 1 are the magnitudes of the first harmonic ($e^{i\omega t}$) coefficients, which resulted from their Fourier analysis of the nonlinear time dependent results. Their analysis also shows that the higher harmonics are quite small in comparison. This is to be expected from the perturbation expansion, which shows that terms involving higher harmonics are of order ϵ^2. This result lends some credence to the linearized approach used here. It is hoped that future improvements in both the small disturbance steady and linearized unsteady perturbation methods will improve certain details of the present results.

B. NACA 64A006 with Control Surface Oscillation

As mentioned in the introduction, the primary application of the method described here is the calculation of generalized unsteady forces for use in flutter studies. Such a study re-

Table 1 Comparison of lift and moment perturbations

			Magnus and Yoshihara[8]	Present results
$k=0$	ΔC_l	0°→2°	0.3841	0.338
		2°→4°	0.3543	
	ΔC_m	0°→2°	0.129	0.115
		2°→4°	0.13	
$k=0.2$	$Re(\Delta C_l)$		0.2385	0.243
	$Im(\Delta C_l)$		−0.1003	−0.096
	$Re(\Delta C_m)$		0.08933	0.0866
	$Im(\Delta C_m)$		−0.03418	−0.0304

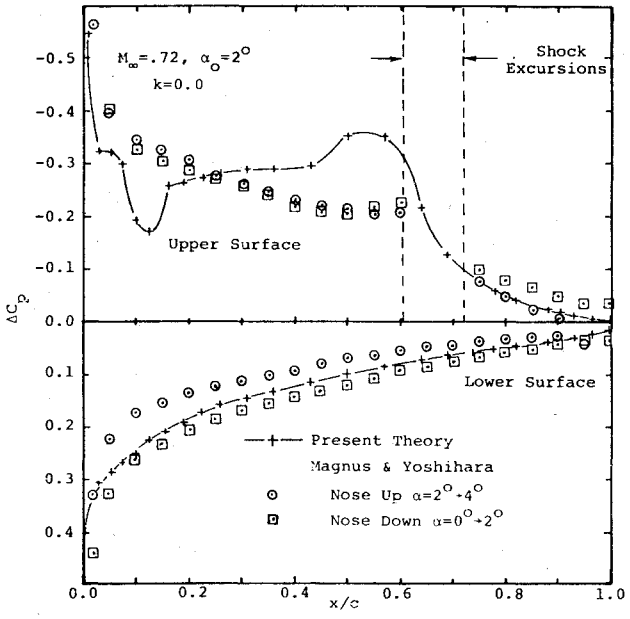

Fig. 3 Magnitude of pressure coefficient perturbations due to a 2° deflection in pitch.

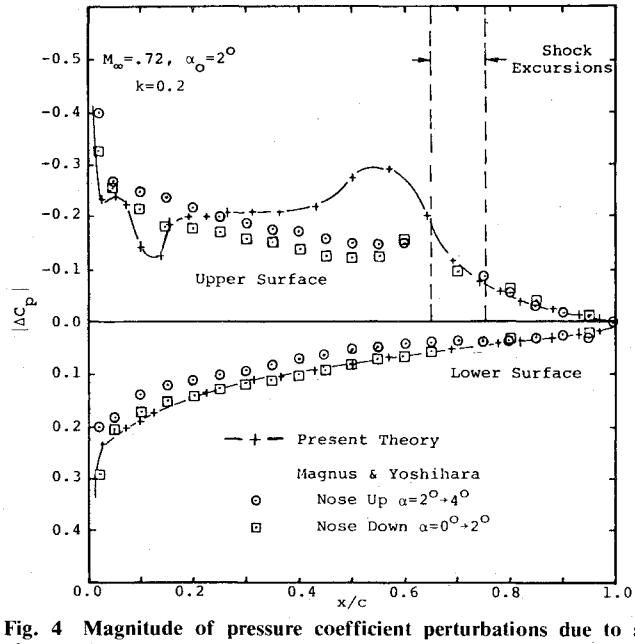

Fig. 4 Magnitude of pressure coefficient perturbations due to a 2° oscillation in pitch.

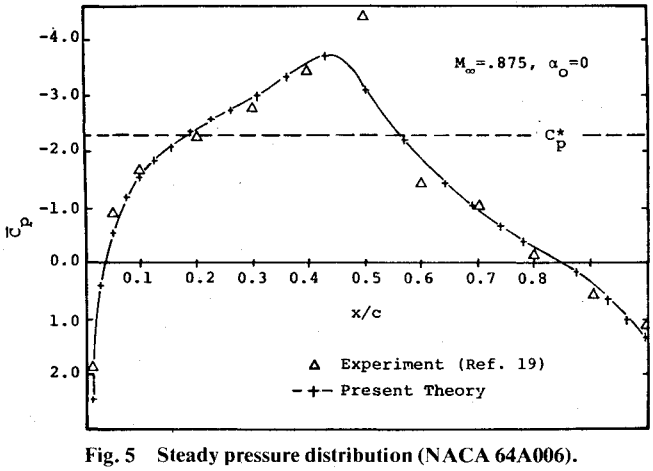

Fig. 5 Steady pressure distribution (NACA 64A006).

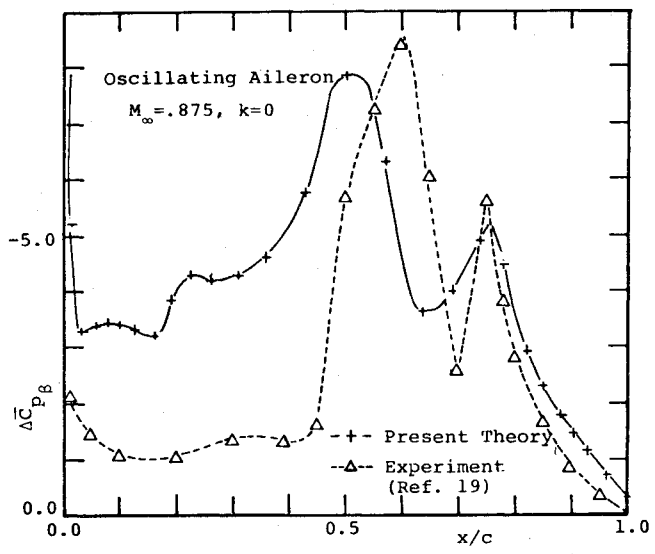

Fig. 6 Scaled pressure perturbation due to aileron deflection.

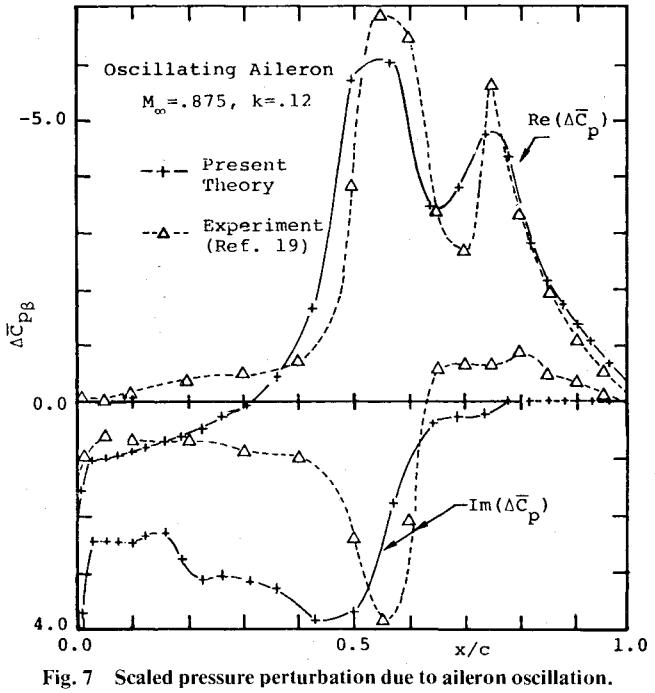

Fig. 7 Scaled pressure perturbation due to aileron oscillation.

cently has been undertaken for the NACA 64A006 airfoil with three rigid body degrees of freedom: pitch, plunge, and control surface oscillation. This required the calculation of unsteady forces and moments in the transonic Mach number range 0.8 to 1.2 for reduced frequencies between 0 and 0.2 for each of the oscillating degrees of freedom. It is noted in passing that the entire matrix of calculations (~110 cases) required approximately 1.25 hr of CDC 7600 time. The flutter calculations are currently in progress and will be reported on in the near future. In this section, some of the results generated for control surface oscillations are presented, with comparison to the experimental data of Tijdeman, Bergh, and Schippers[18,19] for the same airfoil and control surface configuration. It is noted that the experimental technique used to measure unsteady pressures was sensitive only to the first harmonic, so that theory and experiment are being compared on the same bases.

Sample results for airfoil pressure coefficients (in scaled form) for nonlinear steady (Fig. 5) and for linearized perturbations for $k=0$ (Fig. 6) and $k=0.12$ (Fig. 7) are presented in the following. The steady results for a supercritical Mach

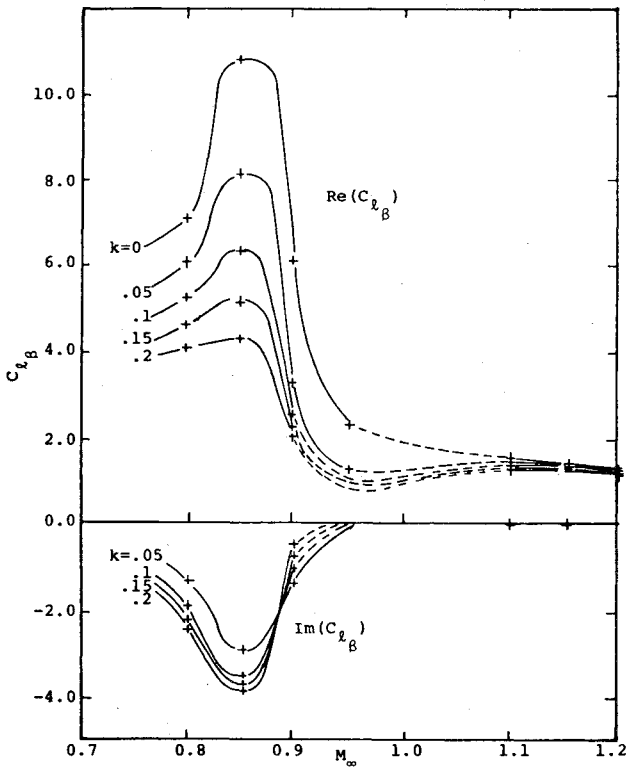

Fig. 8 Lift due to aileron oscillation.

number of 0.875 and zero degree angle of attack show good agreement with experiment, with the exception of the region near the shock. The present small disturbance results show what must be called a rapid compression at about midchord, whereas the data show a diffuse but moderately strong shock. Refinement of the grid between $x/c=0.5$ and 0.6 would most surely enhance the comparison, but it is likely that the use of shock point differencing would over-correct for the rearward position of the shock.

The linearized perturbation results for a steady control surface deflection and for an unsteady control surface oscillation at $k=0.12$ (Figs. 6 and 7) show good qualitative agreement with data. As shown in Fig. 6, the theory overpredicts the pressure perturbation on the stationary forward portion of the airfoil in comparison to the data. This is characteristic of all cases calculated, and is believed to be in part because of the reduced upstream influence resulting from wall effects in the experiment. It is recalled that the present calculations are for free air conditions. Recent preliminary calculations with a solid wall boundary condition show a significant reduction in upstream influence. Other details of the pressure distribution, such as peak suction at the shock (slightly forward of the experimental peak) and hinge point singularity, seem to be well-predicted by the theory. The unsteady $k=0.12$ results in Fig. 7 show a similar qualitative comparison with some significant quantitative differences in magnitude and phase on the forward portion of the airfoil.

Figure 8 presents a summary of results for the real and imaginary parts of the lift coefficient per unit flap deflection (C_{ℓ_β}) as a function of Mach number for various reduced frequencies. The results demonstrate the expected strong nonlinear effects in the transonic regime, as well as the large phase shifts in unsteady forces. Portions of the curves between $M=0.95$ and 1.1 are extrapolated because of the inability to perform stable unsteady calculations in this region. For example, at $M=0.95$, the numerical method was unstable for $k\geq 0.1$ and for all reduced frequencies at $M=1.05$. The required extrapolations are made with some degree of confidence, however, because of the "Mach freeze" effect in this region. That is, steady calculations for $M=0.95$ and 1.05 show only slight differences in the solution field on

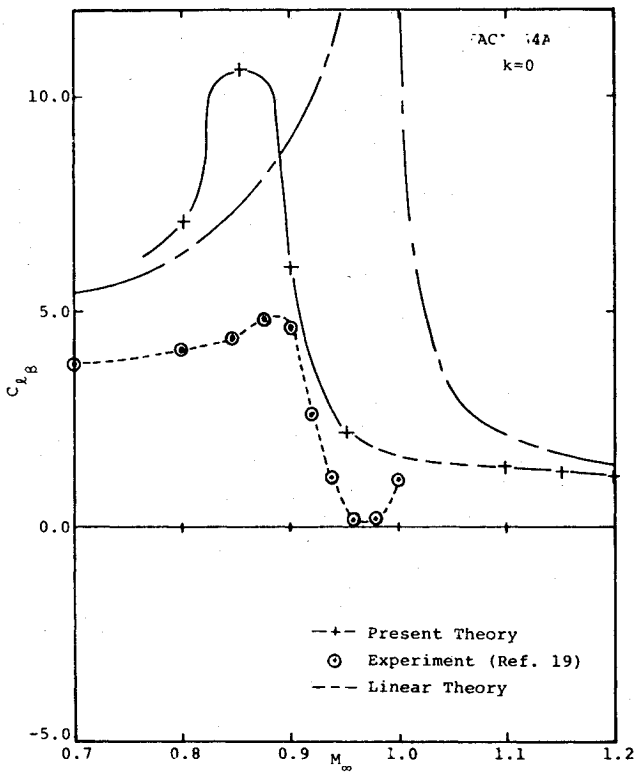

Fig. 9 Lift due to aileron deflection.

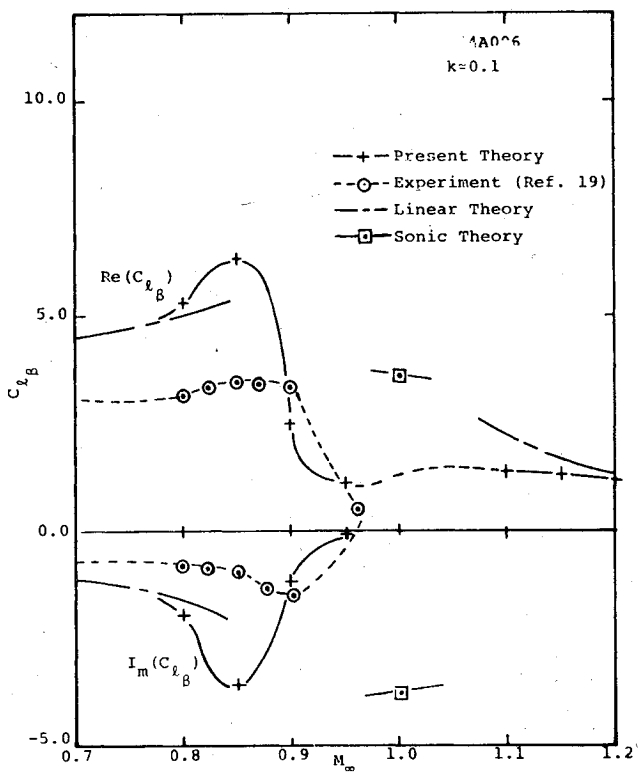

Fig. 10 Lift due to aileron oscillation.

or near the airfoil, so that unsteady control surface perturbations are expected to vary only sightly from the $M=0.95$ or $M=1.1$ results.

Comparisons of the theoretical results for C_{l_β} with experimental data and with linear subsonic/supersonic theory are made in Figs. 9 and 10 for $k=0$ and 0.1, respectively. As shown, the present theory reduces to linear theory away from Mach 1. In each case, the present results are significantly larger than the data, although a qualitative agreement is apparent. The peak in the theoretical results at $M=0.85$ seems to result from a lift augmentation effect due to coalescence at the shock of upstream traveling control surface perturbations. This effect does not occur in linear, uniform flow theory for obvious reasons, and is not in evidence in the data, perhaps because of the reduced upstream influence mentioned previously. One final comment with respect to these comparisons is in order. It is noted that the data are in considerable disagreement with subsonic linear theory (and the present theory) for a fully subcritical Mach number of 0.7. It seems highly probable that the reason for the discrepancy is the existence of a strong viscous effect in the data. The estimated chord Reynolds number of less than 200,000 for the experiments adds further weight to this conclusion. Such effects could only be magnified in the transonic speed range.

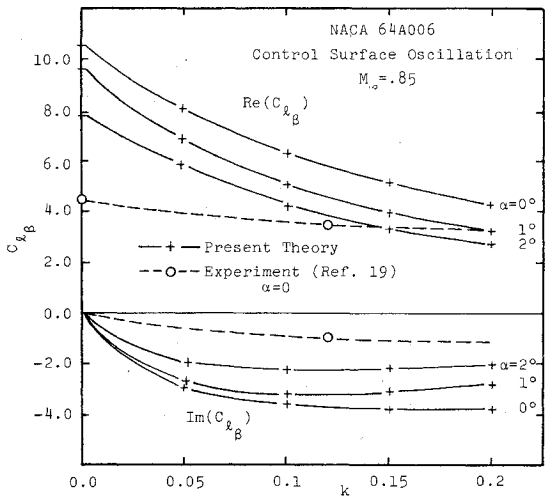

Fig. 11 Mean angle of attack and reduced frequency effect on lift coefficient.

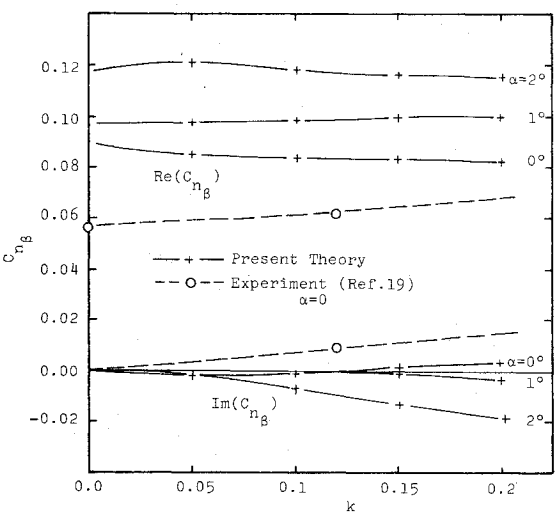

Fig. 12 Mean angle of attack and reduced frequency effect on hinge moment coefficient.

A final set of results are presented in Figs. 11 and 12 for lift and hinge moment coefficients, respectively, as functions of reduced frequency at Mach number 0.85 for various mean angles of attack. Limited experimental data are presented for comparison. The strong reduced frequency effect shown for C_{l_β} and weak dependence for C_{n_β} are consistent with subsonic linear theory. The primary result of note is the prediction of a substantial mean angle of attack effect. Of some considerable interest to the flutter problem is the change in sign of the imaginary (out of phase) part of the hinge moment due to mean angle of attack. This indicates a potential for one-

degree-of-freedom flutter (control surface buzz) solely due to mean airfoil angle of attack, an important result not predicted by linear theory.

IV. Conclusions

In preceding sections, a treatment of unsteady transonic flow as a small perturbation about the nonlinear small disturbance steady flow is presented. The technique has been applied to representative airfoils oscillating at subsonic, through transonic, to supersonic Mach numbers. It is shown that the present theory matches linearized unsteady subsonic or supersonic theory as Mach number decreases, or increases, away from sonic, respectively. The theory includes the effects of thickness and angle of attack, which are ignored in linear theories, but which, as the results presented here demonstrate, are significant in the low-frequency unsteady transonic speed regime. The efficiency of the computational scheme is such that the matrix of calculations required to generate unsteady aerodynamic coefficients for a transonic flutter study of a three-degree-of-freedom, two-dimensional airfoil can be completed in about 1¼ hr of CDC 7600 time.

The results presented here indicate that the theory and numerical solution method provide a meaningful representation of inviscid transonic flows about practical airfoils for reasonable amplitudes of unsteady motion. The results are shown to compare adequately with the "exact" numerical calculations of Magnus and Yoshihara for low-frequency unsteady supercritical flows, for an expenditure of over two orders of magnitude less computer time. Although these comparisons show some qualitative differences in unsteady airfoil pressure perturbations, unsteady aerodynamic forces compare very well in both amplitude and phase. Detailed comparisons of the present results to limited available two-dimensional experimental data show good qualitative agreement. Quantitative discrepancies would seem to be related mainly to viscous effects, not accounted for in the model, and to possible wind-tunnel wall or three-dimensional flow effects in the data.

References

[1] Landahl, M.T., *Unsteady Transonic Flow, International Series of Monographs in Aeronautics and Astronautics,* Pergamon Press, London, 1961.

[2] Rott, N., "Flugelschwingungsformen in Ebener Kompressibler Potential-Stromung," Zeitschrift fur angewandte Mathematik und Physik, Vol. 1, Fasc. 6, 1950.

[3] Landahl, M.T., "Linearized Theory for Unsteady Transonic Flow," *Symposium Transsonicum*, edited by K. Oswatitsch, Springer-Verlag, Berlin.

[4] Nelson, H.C. and Berman, J.H., "Calculations of the Forces and Moments for an Oscillating Wing-Aileron Combination in a Two-Dimensional Potential Flow at Sonic Speeds," NACA Rept. 1128, 1953.

[5] Stahara, S.S. amd Spreiter, J.R., "Development of a Nonlinear Unsteady Transonic Flow Theory," NASA CR-2258, June 1973.

[6] Isogai, K., "Unsteady Transonic Flow Over Oscillating Circular-Arc Airfoils," AIAA Paper 74-360, Las Vegas, Nev., 1974.

[7] Magnus, R. and Yoshihara, H., "Inviscid Transonic Flow Over Airfoils," *AIAA Journal*, Vol. 8, Dec. 1970, pp. 2157-2162.

[8] Magnus, R. and Yoshihara, H., "Calculations of Transonic Flow Over an Oscillating Airfoil," AIAA Paper 75-98, Pasadena, Calif., 1975.

[9] Beam, R.M. and Warming, R.F., "Numerical Calculations of Two Dimensional, Unsteady Transonic Flows with Circulation," NASA TN D-7605, Feb. 1974.

[10] Ballhaus, W.F. and Lomax, H., "The Numerical Simulation of Low Frequency Unsteady Transonic Flow Fields," *Proceedings of the Fourth International Conference on Numerical Methods in Fluid Dynamics, Vol. 35, Lecture Notes in Physics,* Springer-Verlag, Berlin, 1974, pp. 57-63.

[11] Ballhaus, W.F., Magnus, R., and Yoshihara, H., "Some Examples of Unsteady Transonic Flows Over Airfoils," Symposium on Unsteady Aerodynamics, Tucson, Ariz., March 1975.

[12] Bratanow, T. and Ecer, A., "Computational Considerations in Application of the Finite Element Method for Analysis of Unsteady Flow around Airfoils," AIAA Computational Fluid Dynamics Conference, Palm Springs, Calif., July 1973.

[13] Chan, S.T.K. and Brashears, M.R., "Finite Element Analysis of Transonic Flow," Air Force Flight Dynamics. Laboratory, Wright-Patterson Air Force Base, Ohio, AFFDL-TR-74-11, March 1974.

[14] Murman, E.M. and Cole, J.D., "Calculation of Plane Steady Transonic Flows," *AIAA Journal,* Vol. 9, Jan. 1971, pp. 114-121.

[15] Murman, E.M. and Krupp, J.A., "The Numerical Calculations of Steady Transonic Flows Past Thin Lifting Airfoils and Slender Bodies," AIAA Paper 71-566, Palo Alto, Calif., 1971.

[16] Ehlers, F.E., "A Finite Difference Method for the Solution of the Transonic Flow Around Harmonically Oscillating Wings," AIAA Paper 74-543, Palo Alto, Calif., 1974.

[17] Traci, R.M., Albano, E.D., Farr, J.L., and Cheng, H.K., "Small Disturbance Transonic Flows About Oscillating Airfoils," Air Force Flight Dynamics Laboratory, Wright-Patterson Air Force Base, Ohio, AFFDL-TR-74-37, June 1974.

[18] Tijdeman, H. and Bergh, H., "Analysis of Pressure Distributions Measured on a Wing With Oscillating Control Surface in Two-Dimensional High Subsonic and Transonic Flow," NLR-TR-F. 253, 1967.

[19] Tijdeman, H. and Schippers, P., "Results of Pressure Measurements on an Airfoil with Oscillating Flap in Two-Dimensional High Subsonic and Transonic Flow," Provisional Issue, NLR TR 730-78 U, Aug. 1973.

[20] Farr, J.L., Traci, R.M., and Albano, E.D., "Computer Programs for Calculating Small Disturbance Transonic Flows About Oscillating Airfoils," Air Force Flight Dynamics Laboratory, Wright-Patterson Air Force Base, Ohio, AFFDL-TR-74-135, Nov. 1974.

[21] Murman, E.M., "Analysis of Embedded Shock Waves Calculated by Relaxation Methods," *AIAA Journal*, Vol. 12, May 1974, pp. 626-633.

[22] Hafez, M.M. and Cheng, H.K., "Convergence Acceleration and Shock Fitting for Transonic Aerodynamics Computation," AIAA Paper 75-51, Pasadena Calif., 1975.